Available online at www.sciencedirect.com
ScienceDirect
Journal of Colloid and Interface Science 315 (2007) 761–767
JOURNAL OF Colloid and Interface Science
www.elsevier.com/locate/jcis

Nonideal mixed micelles of Gemini surfactant homologues and their application as templates for mesoporous material MCM-48

Jun Hu, Lihui Zhou, Jian Feng, Honglai Liu *, Ying Hu

State Key Laboratory of Chemical Engineering and Department of Chemistry, East China University of Science and Technology, Shanghai 200237, People's Republic of China

Received 6 April 2007; accepted 29 June 2007

Available online 20 August 2007

Abstract

The micellization properties of aqueous solutions of the mixed Gemini surfactant homologues GEM16-6-16 and GEM16-12-16 with various compositions were investigated. The measured critical micelle concentration (CMC) deviated significantly from the ideal mixing model. Good agreement was found with a nonideal mixing model, the Margules model, which has two optimal parameters, $A_{12} = -3.611$ and $A_{21} = -6.318$. It was shown that the properties of mixed micelles were not sensitive to the compositions, and most of the GEM16-12-16 molecules were aggregated into the micelles. Dynamic laser light-scattering measurements revealed that the mixed micelles had almost the same size and similar zeta potential. When the mixed micelles were used as templates, a series of highly ordered cubic MCM-48 mesoporous materials, characterized by XRD and TEM, were produced through self-assembly. The N_2 adsorption–desorption measurements suggested that the pores of these materials had similar average diameters of 2.2–2.5 nm. This further demonstrated the nonideal behavior of the homologue mixture.

Keywords: Gemini surfactant homologues; Mixed micelles; Pseudo-phase separation model; Template; MCM-48

1. Introduction

In recent years, Gemini surfactants have attracted considerable attention due to their special physicochemical properties, especially their lower CMC and efficient ability to lower surface tension [1–4]. Typical examples are cationic quaternary ammonium Gemini homologues, which have two identical amphiphilic moieties connected at the level of the head groups by a spacer group. Mixed micelles composed of surfactant homologues with the same hydrophilic group are usually assumed to obey ideal mixing [5–7]. So previous studies of synergistic interactions between Gemini and other surfactants have mainly focused on conventional ionic or nonionic surfactants [8–18], and most of them have treated the mixed micelles system via a pseudo-phase separation model and the regular solution theory [19,20] with only one parameter, β [11,14–18]. However, the choice of a symmetric function in the composition as $\Delta G^{E}_{mix} = \beta RT x_1 x_2$ usually causes the two species' activity coefficients with each other to be mirror images, and it is hard to provide a satisfactory representation of nonideality for complicated systems. Moreover, studies relating to the interactions between the Gemini homologues are rather few.

On the other hand, the applications of the Gemini surfactants have been widely explored. The most notable one is their template functions in the discovery of mesoporous materials: M41S [21,22]. After that, a wide range of new mesostructure materials has been developed using the surfactant template technology [23,24]. Since the configurations and properties of the Gemini micelles are adjustable by their different lengths of tails and various groups of spacers [25], by the self-assembly template approach [22,26], the structures of mesoporous materials can be considerably affected. Both Stucky and co-workers [27] and van der Voort et al. [28] elucidated that the spacer length of the Gemini surfactants can influence the crystallographic phase of mesoporous materials—the longer spacer yields cubic MCM-48 while the shorter one favors hexagonal MCM-41. In our previous work, similar results have been obtained that bis(hexadecyldimethylammonium) hexane (GEM16-6-16) is a good template for MCM-41, while

* Corresponding author. Fax: +86 21 64252921.
E-mail address: hlliu@ecust.edu.cn (H. Liu).

0021-9797/$ – see front matter
doi:10.1016/j.jcis.2007.06.077

bis(hexadecyldimethylammonium) dodecane (GEM16-12-16) is for MCM-48 [29]. It clearly appears that the interaction between the inorganic precursor and the template is a key factor in the control of the material mesostructure. Stucky and co-workers [30] rationalized the synthesis of MCM-48 by carefully selecting a mixture of GEM16-12-16 and GEM16-3-1, where GEM16-12-16 was the main component in the mixed micelles while the other was the co-surfactant. Kao et al. [31] found that the use of the Gemini surfactant facilitated the synthesis of Al-MCM-48 without compromising the integrity of the cubic mesostructure. More recently, Li and co-workers [32] studied the influence of a binary mixture of cationic and anionic surfactants on the synthesis of Fe-MCM-48. Zhao and co-workers synthesized ordered bimodal mesoporous silica materials by using templates of two dimension size micelles, which coexisted in the system at the same time [33]. However, the step where such interactions occur is still open to investigate and appears to depend strongly on the synthesis conditions.

In this work, we investigate the micellization behavior of mixed Gemini homologues of GEM16-6-16 and GEM16-12-16 and their template approaches for preparing mesoporous structures. We adopted the Margules model, which has two parameters, A_{12} and A_{21}, to predict the excess mixing Gibbs energy and the mixed micelle compositions. Moreover, we used mixed micelles with stepwise changing composition as templates to synthesize a series of mesoporous materials. Combining the evidences, we tentatively elucidated the synergism of these two Gemini homologues and their template approaches for MCM-48.

2. Experimental

2.1. Synthesis

Gemini surfactants were prepared by refluxing α,ω-dibromohexane (or α,ω-dibromo dodecane) and excessive N,N-dimethylhexadecylamine in dry ethanol solution for 2–4 d, followed by more than three recrystallizations from a mixture of ethanol and acetic ether [34]. Both products had satisfactory ^{1}H NMR spectra, which were characterized on a Brucker Avance-500 system with $CdCl_3$ as the solvent.

The surfactants were completely dissolved in water at 313 K with vigorous stirring. NaOH was then added at room temperature, and after a few minutes tetraethyl orthosilicate (TEOS) was dripped. The molar composition of the mixture gel was (TEOS:GEM:NaOH:H_2O) = (1:0.06:0.6:100). After being stirred for 3 h, the entire gel solution was put into an autoclave at 373 K for 2–5 d. The white as-synthesized solid was obtained by vacuum filtration and washed with water and ethanol. Finally, the products were calcined at 823 K for 6 h in ambient air, with a heating rate of 2 K min^{-1}.

2.2. Characterization

The CMCs of surfactant solutions at 298 K were determined by a surface tension method on a ThermoCahn DCA-315 contact-angle surface-tension analysis system. The size distribution and zeta potential of micelles were determined by a dynamic laser light-scattering (DLS) technique on Malvern Nano-ZS.

Powder XRD measurements were carried out on a D/Max-2550 VB/PC diffractometer (40 kV, 200 mA), using Cu$K\alpha$ radiation. Transmission electron micrographs (TEM) were taken on a JEOL JEM-2010. The samples were dispersed in ethanol solution and supported on copper grids. The scanning electron microscope (SEM) images were observed on a JEOL JSM-6360-LV with conventional sample preparation. The nitrogen adsorption–desorption isotherms were collected at liquid nitrogen temperature over a range of relative pressures from 0.01 to 0.995 on an ASAP-2010 volumetric adsorption analyzer. The BJH model was used to determine the pore diameter and the pore size distribution.

3. Model

The pseudo-phase separation model of nonideal binary mixed micelles gives a simple relation between the CMC of the mixed surfactants (C_{12}) and that of each pure surfactant i (C_1, C_2),

$$\alpha_i C_{12} = x_i \gamma_i C_i, \tag{1}$$

where α_i, x_i are the mole fractions of the surfactant i in the mixed solutions and micelles, and subject to the constraints $\sum_{i=1}^{2} \alpha_i = 1$, $\sum_{i=1}^{2} x_i = 1$, respectively. γ_i is the activity coefficient of the surfactant i in the mixed micelles. According to the two-parameter Margules model, the activity coefficient γ_i can be expressed as a function of the mole fraction x_i and the parameters A_{12} and A_{21} [35,36]:

$$\ln\gamma_1 = \big[A_{12} + 2(A_{21} - A_{12})x_1\big]x_2^2, \tag{2}$$

$$\ln\gamma_2 = \big[A_{21} + 2(A_{12} - A_{21})x_2\big]x_1^2. \tag{3}$$

The parameters A_{12} and A_{21} can be initially estimated by $A_{12} \propto b_1/RT$, $A_{21} \propto b_2/RT$, where b_i is the van der Waals volume parameter. In this work, they would be expected to respond to the different spacer lengths of the homologous surfactants 1 (GEM16-6-16) and surfactant 2 (GEM16-12-16).

According to Eq. (1), we make a substitution of γ_i in Eqs. (2) and (3), and therefore

$$\ln(\alpha_1 C_{12}/C_1) = \ln x_1 + \big[A_{12} + 2(A_{21} - A_{12})x_1\big]x_2^2, \tag{4}$$

$$\ln(\alpha_2 C_{12}/C_2) = \ln x_2 + \big[A_{21} + 2(A_{12} - A_{21})x_2\big]x_1^2. \tag{5}$$

From the constraint $\sum_{i=1}^{2} x_i = 1$ and Eq. (1), we have

$$\frac{\alpha_1 C_{12}}{\gamma_1 C_1} + \frac{\alpha_2 C_{12}}{\gamma_2 C_2} = 1. \tag{6}$$

Thus, the excess Gibbs free energy G^{E} can be calculated as [37]

$$G^{\mathrm{E}} = RT[A_{12}x_2 + A_{21}x_1]x_1x_2. \tag{7}$$

Combining Eqs. (4)–(6), we can iteratively evaluate the values of parameters A_{12} and A_{21} of the binary system from the experimental data of C_1, C_2, and C_{12} at various mole fractions a_1. Hence, we can predict the properties of the mixtures,

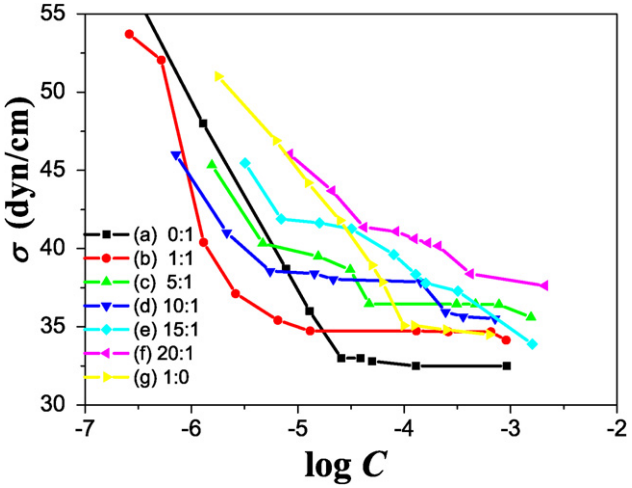

Fig. 1. The concentration dependence of the surface tension σ of the mixed solutions with different molar ratios of GEM16-6-16 and GEM16-12-16 at 298 K.

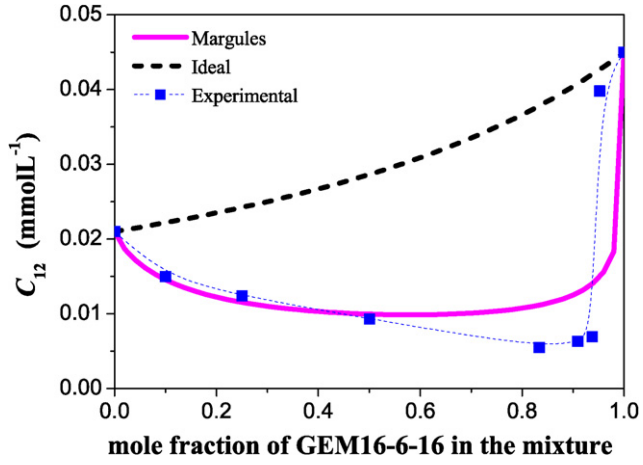

Fig. 2. The variation of the CMC of the GEM16-6-16 and GEM16-12-16 mixed solutions with the composition of the surfactant mixtures. Solid squares are experimental data, dashed line is the prediction of the ideal mixing model, and solid line is the prediction of the nonideal mixing model with $A_{12} = -3.611$ and $A_{21} = -6.318$.

such as C_{12}, x_1, and G^{E}, at any given composition and then make a conclusion as to whether the mixing is ideal or not.

4. Results and discussion

4.1. Nonideal mixed micelles of homologues GEM16-6-16 and GEM16-12-16

The variations of the surface tension of the GEM16-6-16 and GEM16-12-16 mixed solutions with different molar ratios $R_{6\text{–}12}$ as a function of the logarithm of the total surfactant mixture concentrations are shown in Fig. 1. The experimental value of the CMC of pure GEM16-6-16 ($\log C_1 = -4.00$) in the curve (g) is higher than that of pure GEM16-12-16 ($\log C_2 = -4.29$) in the curve (a); therefore, the latter can form micelles more easily than the former. When they are mixed together, as shown in the curve (b) with $R_{6\text{–}12} = 1{:}1$ ($\alpha_1 = 0.5$), they present a signal discontinuity at $\log C_{12} = -4.90$; while for the various $R_{6\text{–}12}$ of 4:1, 9:1, 15:1, and 20:1 (corresponding to α_1 of 0.80, 0.90, 0.933, and 0.95), each mixture curve (c–f) has two discontinuities. The logarithm of the first discontinuity concentration is in the range from -4.5 to -5.2, and the second one is from -3.5 to -4.0. The possible explanation is that with a relatively large number of GEM16-6-16 molecules in the dilute mixed solutions, the GEM16-12-16 molecules can cluster together at even lower concentration, so all the first CMCs of the mixtures are smaller than those of pure surfactants, and hence, the GEM16-12-16 molecules may dominate in the mixed micelles. With further increase of the mixture concentration, most of the GEM16-6-16 molecules, together with the GEM16-12-16 molecules, cluster together to form stable mixed micelles, and the second discontinuities occur.

The variation of the first discontinuity concentration C_{12} as a function of the composition of the surfactant mixture is shown in Fig. 2 as solid squares. It indicates that when a small amount of GEM16-12-16 is added into the GEM16-6-16 solution, the C_{12} decreases sharply; then it remains at a nearly constant value with further increase in the amount of GEM16-12-16. The dashed line in Fig. 2 is the prediction of the Clint relation [7] based on the hypothesis of ideal mixing as Eq. (8):

$$1/C_{12} = \alpha_1/C_1 + (1-\alpha_1)/C_2. \tag{8}$$

The ideal mixing line deviates from the experimental values significantly. The solid line in Fig. 2 is the prediction of the Margules model with the optimal parameters $A_{12} = -3.611$ and $A_{21} = -6.318$. It shows that the nonideal mixing model gives much better agreement with the experimental values; therefore, the mixing behavior of the homologues GEM16-6-16 and GEM16-12-16 is nonideal.

In aqueous solutions, strong Coulombic repulsion between the two positively charged head groups within a surfactant unit makes the spacer chain fully stretched; however, the unfavorable contact with water makes it shrink to the hydrophobic nucleus. Therefore, a critical distance between the two head groups will result to balance these two opposing tendencies. Bhattacharya and his co-workers reported that the critical distances between the two head groups of pure GEM16-6-16 and GEM16-12-16 are 11.0 and 14.0 Å, and hence, the volumes are about 1320 and 1880 Å^3, respectively [25]. Because the ratio of the parameters A_{21}/A_{12} is proportional to the ratio b_2/b_1, where b_i is the van der Waals volume parameter, the validity of the prediction of A_{12} and A_{21} could be evaluated through the ratio of volumes of surfactant molecules. Since $V_2/V_1 = 1.42$, the values of A_{21} and A_{12} are quite reasonable.

The variation of the mole fraction of GEM16-6-16 in the mixed micelle, x_1, as a function of the composition of the surfactant mixtures, α_1, was calculated from Eqs. (4) and (5) with the optimal parameters $A_{12} = -3.611$ and $A_{21} = -6.318$. The results shown in Fig. 3 suggest that the mole fraction x_1 increases rapidly first when α_1 is less than 0.1, and then it slows down, but when α_1 is greater than 0.90, x_1 increases rapidly again. In the right region of the cross-point ($x_1 = 0.40$), we can see that the concentration of GEM16-6-16 in the mixed micelle, x_1, is always lower than that in the mixture, α_1. For example, when $R_{6\text{–}12}$ is equal to 4:1 ($\alpha_1 = 0.8$), the mole fraction in

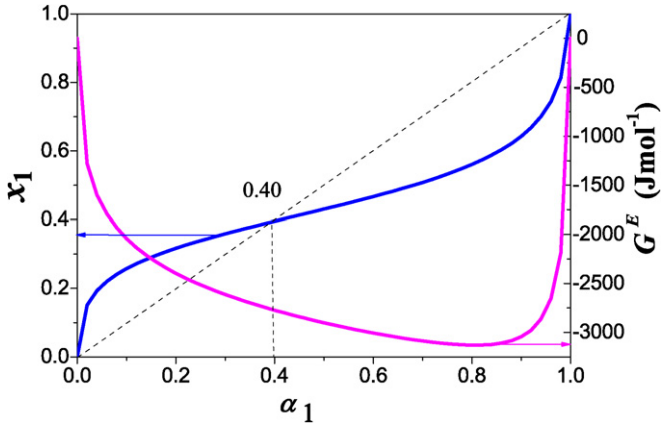

Fig. 3. Variations of the mole fraction of GEM16-6-16 in the mixed micelles and the excess Gibbs free energy as functions of the composition of the surfactant mixtures.

Table 1
Size and zeta potential distributions by LLS with different ratios R_{6-12}

Ratio R_{6-12}[a]	Size (nm)	Zeta potentials (mV)
0	6	31.20
1	6	29.6
5	5	20.95
10	6	23.24
15	5	23.42
20	5	24.40
∞	5	26.84

[a] The surfactant mixture solutions were prepared under the same conditions of synthesis of mesoporous materials before the titration of TESO.

the mixed micelle x_1 is equal to 0.54, which means that there are many more GEM16-12-16 molecules in the mixed micelle ($x_2 = 0.56$) than in the mixed solution ($\alpha_2 = 0.2$). The reason may lie in the structure of the micelles. There might be a concentration distribution inside the micelles. The GEM16-12-16 molecules would be concentrated in the surface region of the micelle because of the lower surface energy. The GEM16-6-16 molecules are more favorable to staying in the inner part. The surface is therefore constructed by a majority of GEM16-12-16 mixed with a small part of GEM16-6-16, which makes the structure of micelles more stable than that formed by the pure species. This is very similar to the role of the co-surfactant in the formation of microemulsions.

The excess Gibbs free energy G^{E} was calculated from Eq. (7) and plotted in Fig. 3. The negative G^{E} suggests that the GEM16-6-16 and GEM16-12-16 molecules have stronger interactions with each other, and the synergic effect stabilize the mixed micelles. Additionally, the size distribution and zeta potential of the mixed micelles determined by DLS are shown in Table 1. The mixed micelles, with R_{6-12} of 1:1, 4:1, 9:1, 15:1, and 20:1, have approximately the same size of 5–6 nm and similar zeta potentials of 20–30 mV. The results indicate that the micellization process of the homologue mixtures is not sensitive to the compositions and the ionic degree, hence the surface charge densities of the mixed micelles are similar.

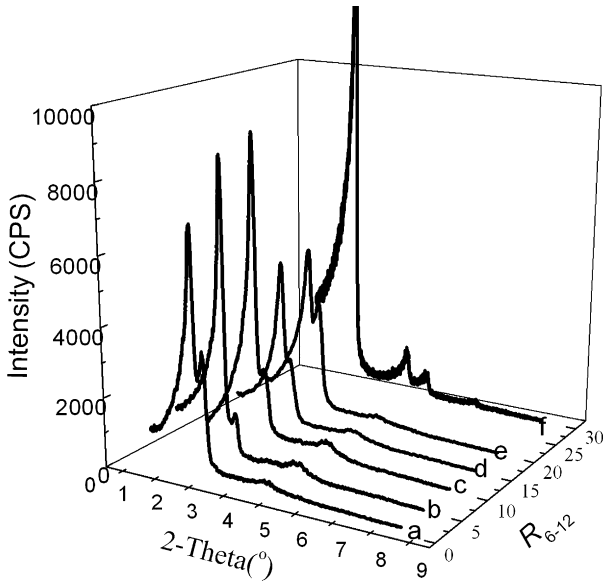

Fig. 4. The XRD patterns of mesoporous materials produced by GEM16-6-16 and GEM16-12-16 mixture templates with different ratios. (The total molar ratio of surfactants to TEOS is held constant as 0.06.) (a) $R_{6-12} = 1{:}1$, (b) $R_{6-12} = 5{:}1$, (c) $R_{6-12} = 10{:}1$, (d) $R_{6-12} = 15{:}1$, (e) $R_{6-12} = 20{:}1$, (f) pure GEM16-6-16.

4.2. Structure of mesoporous materials prepared using Gemini surfactant mixture as the template

The GEM16-6-16 and GEM16-12-16 homologous mixtures, with various ratios of R_{6-12}, have been used as templates to synthesize a series of mesoporous materials. The XRD patterns of the products are shown in Fig. 4. Among the diffraction curves, curve (a) is for the calcined product produced by the mixture with molar ratio R_{6-12} of 1:1. It has an intense reflection peak and a small peak on its shoulder at $2\theta = 2.276°$ and 2.578°, and the corresponding ratio of $1/d$ is $\sqrt{3}{:}2$, which would be assigned to the 211 and 220 reflection planes, respectively. The other small reflections are present at $2\theta = 4.315°$ and 4.453°, respectively. This is a typical pattern of the cubic arrangements of MCM-48. The well-resolved cubic structure is further confirmed by TEM images with different orientations and their FFT diffraction graphs. Fig. 5a shows the image of square lattices along the 110 direction, Fig. 5b shows the image of hexagonal lattices along the 111 direction, and Fig. 5c shows the image of quadrate-rod lattices along the 311 direction, respectively. Combining all these observations gives further evidence that this mixture template produces a high-quality $Ia\bar{3}d$ cubic mesoporous material of MCM-48. Even more, when the ratio R_{6-12} of the surfactant mixture templates is stepped up to 5:1, 10:1, 15:1, and extremely 20:1, all the synthesized mesoporous materials have similar XRD patterns, as shown in Figs. 4b–4e. Each diffraction pattern has clear double reflections in the range of $2\theta = 2.3°$–$2.8°$, which reflects the characteristics of cubic mesoporous structure.

The N_2 adsorption–desorption isotherms of all these mesoporous products are shown in Fig. 6a. For the ratio $R_{6-12} \leqslant 5$, the adsorption–desorption isotherm curves (a–c) exhibit type IV isotherm behavior, which indicates the presence of a meso-

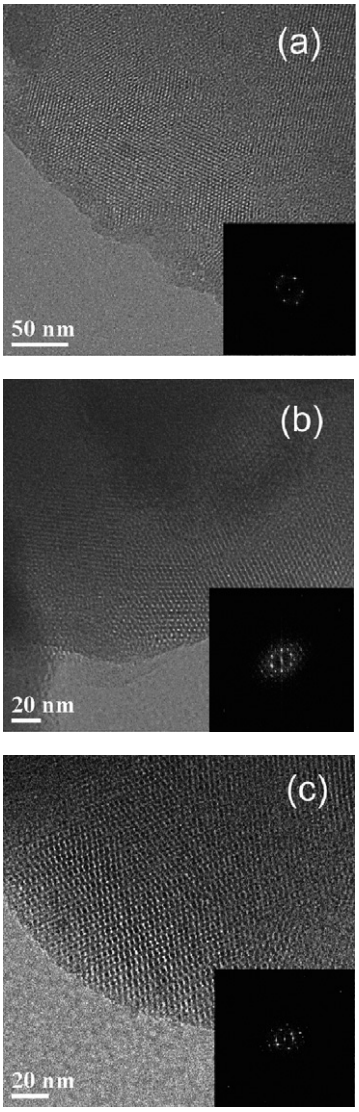

Fig. 5. The TEM images of mesoporous materials produced by GEM16-6-16 and GEM16-12-16 mixture template with $R_{6-12} = 1{:}1$: (a) (110) direction, (b) (111) direction, (c) (311) direction. Corresponding FFT diffraction graphs are inserted into each image.

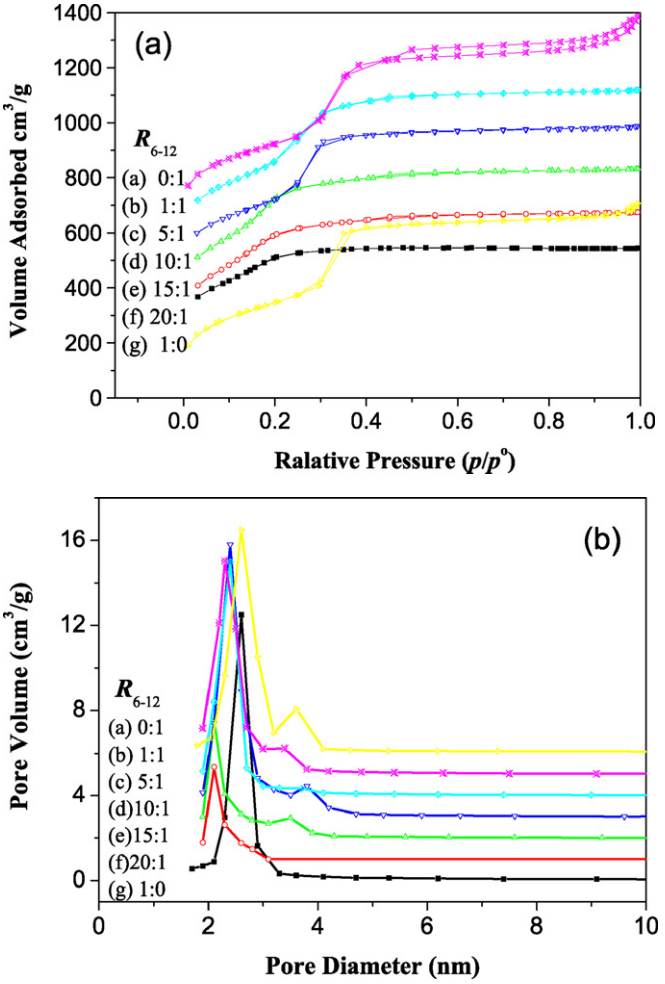

Fig. 6. (a) The N_2 adsorption–desorption isotherms. The scale is shifted by 100 cm^3/g per curve. (b) The pore size distribution calculated by the BJH model based on desorption curves. The scale is shifted by 1 cm^3/g per curve.

porous structure. For the ratio $R_{6-12} \geqslant 10$, the adsorption–desorption isotherm curves (d–f) change to type I behavior, which indicates that the pore size becomes smaller. The size distributions of mesoporous products calculated by the BJH model on desorption curves are shown in Fig. 6b; the two-peak distributions suggest that there are two different size channels in the products: most of them have average size 2–3 nm, only a few about 3.5 nm. The characteristic data for the surface area (S), the BJH cumulative pore volume (V_{BJH}), the BJH average pore diameter (D_p), and the unit cell parameter (a) are listed in Table 2. We can see that no matter what the ratios of R_{6-12} are, the products have the same a of 8.8 nm and similar D_p of 2.2–2.7 nm.

In the mixture templates, GEM16-6-16 is the main component, especially in the last case at $R_{6-12} = 20$, where the molar ratio of GEM16-12-16 to silica is only 0.003 while that of GEM16-6-16 is 0.06, almost the same ratio as in the case of the pure GEM16-6-16 template approach for the hexagonal MCM-41. However, the mesoporous structures of the products based upon these mixture templates do not have a hexagonal structure. In contrast, they have formed the cubic structure of MCM-48, which is characteristically originated by the GEM16-12-16 template. This may be due to the GEM16-12-16 molecules inclining to the surface region of the mixed micelles.

The packing parameter, $p = V/al$, where V and a are the volume and surface area of the surfactant hydrophilic group and l is the critical length of the hydrophobic tail in the fully extended conformation, is closely related to the morphology of the micelle. According to the self-assembly mechanism [21,26], it is also a useful molecular structure-directing index for the porous geometrical characteristics. For the GEM16-6-16 and GEM16-12-16 mixed micelles, both hydrophobic tails are the same; hence, l is independent of the mixture's composition. The surface area a can be obtained from $a = (N_A \Gamma)^{-1}$, where Γ is the surface excess. The surface excess Γ can be calculated from the Gibbs isotherm $\Gamma = -\frac{(d\sigma/d\log c)}{2.303nRT}$ by plotting the surface tension, σ, against $\log c$, and n is a constant of 3 for Gemini surfactants [38]. As shown in Fig. 1, each curve has a similar slope of σ against $\log c$, so the surface area of the mixed

Table 2
The characteristic data of mesoporous materials templated by GEM16-6-16 and GEM16-12-16 mixtures with different ratios of R_{6-12}

R_{6-12}	Mesostructure	S ($m^2\ g^{-1}$)	V_{BJH} ($cm^3\ g^{-1}$)	D_p (nm)	a (nm)
0	Cubic	1495[a]	1.22	2.3	7.6
1	Cubic	1334[a]	1.09	2.4	8.8
5	Cubic	1191[a]	1.02	2.4	8.8
10	Cubic	2742[b]	1.08	2.7	8.7
15	Cubic	2344[b]	0.64	2.4	8.8
20	Cubic	1840[b]	0.38	2.2	8.8
∞	Hexagonal	1208[a]	1.10	2.8	4.7

Note. S is the surface area [a]calculated by BET isotherm and [b]calculated by Langmuir isotherm. V_{BJH}: the cumulative pore volume by BJH model by the desorption curve; D_p: BJH average pore diameter; a: the unit cell parameter—for cubic structure $a = 6^{1/2}d_{211}$, for hexagonal $a = 2 \cdot 3^{-1/2}d_{100}$.

micelles is almost the same. From the above data in Table 1, we can see that the volume of the mixed micelles is nearly constant. Therefore, the packing parameter p of the homologue mixtures, and hence the mesoporous geometrical structures, are not sensitive to the ratios R_{6-12}.

From the above discussion, we can see that GEM16-12-16 has a lower CMC, and the mole fraction of GEM16-12-16 is always higher in the mixed micelle than that in the mixture solution, so the mixed micelles will mostly exhibit the properties of GEM16-12-16. Used as templates, they may have a similar directing approach in the formation of mesoporous products: the homologous molecules aggregate to form mixed micelles with a particular morphology first. Thus, the mixed micelles with similar surface charge densities would absorb similar numbers of counterions of silica oligomers through electrostatic force and self-assemble to the spatially cubic structure in the growth of mesoporous products, finally.

5. Conclusions

It has been shown clearly that the homologous GEM16-6-16 and GEM16-12-16 mixtures are nonideal mixing. All the CMCs of the mixtures were lower than those of pure species, and the other properties, such as micelle size and zeta potential, were not sensitive to the initial composition of the mixture. The nonideal mixing behavior has been satisfactorily described by the Margules model with two optimal parameters, $A_{12} = -3.611$ and $A_{21} = -6.318$. The predicted results of the negative excess mixing Gibbs energy, as well as the composition changes in the mixed micelle, suggested there were synergism effects in the mixed micelles, which were consistent with the nonideal mixing assumption. The Margules model can provide a more efficient way to present the nonideality for complicated systems.

The mixed micelle templates facilitated the synthesis of MCM-48 and improved the quality of the obtained materials. With the different R_{6-12} of 1:1, 5:1, 10:1, 15:1, and extremely 20:1, all the mixed micelles were in favor of directing a cubic structure of MCM-48. The abnormal template approaches can be understood as the cooperative self-assembly effect that the GEM16-12-16 molecules inclining to the surface region of the micelles would result in the similar packing parameter p of the mixed micelles, and hence direct a similar cubic mesoporous structure. These results supported the evidence of nonideal mixing of homologous GEM16-6-16 and GEM16-12-16 on the other hand. Further, they suggest an important pathway in directing the desired material.

Acknowledgments

This work is supported by the National Natural Science Foundation of China (Projects 20490204, 20606010), the Foundation of Shanghai Key Laboratory of Molecular Catalysts and Innovative Materials, Fudan University (Project 2005KF01), and the Shanghai Municipal Science and Technology Commission of China (No. 05DJ14002).

References

[1] C.A. Bunton, L. Robinson, J. Shaak, M.F. Stam, J. Org. Chem. 36 (1971) 2346.
[2] R. Zana, M. Benrraou, R. Rueff, Langmuir 7 (1991) 1072.
[3] M.J. Rosen, Z.H. Zhu, T. Gao, J. Colloid Interface Sci. 157 (1993) 254.
[4] F.M. Menger, C.A. Littau, J. Am. Chem. Soc. 113 (1991) 1451.
[5] H. Lange, Kolloid-Z. 131 (1953) 96.
[6] K. Shinoda, J. Phys. Chem. 58 (1954) 541.
[7] J.H. Clint, J. Chem. Soc. Faraday Trans. I 71 (1975) 1327.
[8] M.J. Rosen, T. Gao, Y. Nakatsuji, A. Masuyama, Colloids Surf. A Physicochem. Eng. Aspects 88 (1994) 1.
[9] L. Liu, M.J. Rosen, J. Colloid Interface Sci. 179 (1996) 454.
[10] R.G. Alargova, I.I. Kochijashky, M.L. Sierra, K. Kwetkat, R. Zana, J. Colloid Interface Sci. 235 (2001) 119.
[11] M.S. Bakshi, K. Singh, J. Colloid Interface Sci. 287 (2005) 288.
[12] D. Danino, Y. Talmon, R. Zana, J. Colloid Interface Sci. 185 (1997) 84.
[13] K.S. Sharma, C. Rodgers, R.M. Palepu, A.K. Rakshit, J. Colloid Interface Sci. 268 (2003) 482.
[14] R.E. Balzhiser, M.R. Samuels, J.D. Eliassen, Chemical Engineering Thermodynamics, Prentice Hall, Englewood Cliffs, NJ, 1972, Chap. 9.
[15] Q. Zhou, M.J. Rosen, Langmuir 19 (2003) 4555.
[16] M.S. Bakshi, J. Singh, K. Singh, G. Kaur, Colloids Surf. A Physicochem. Eng. Aspects 237 (2004) 61.
[17] R. Zhang, L. Zhang, P. Somasundaran, J. Colloid Interface Sci. 278 (2004) 453.
[18] P.C. Schulz, J.L. Rodríguez, R.M. Minardi, M.B. Sierra, M.A. Morini, J. Colloid Interface Sci. 303 (2006) 264.
[19] D.N. Rubingh, in: K.L. Mittal (Ed.), Solution Chemistry of Surfactants, vol. 1, Plenum, New York, 1979, p. 337.
[20] R.F. Kamrath, E.I. Franses, J. Phys. Chem. 88 (1984) 1642.
[21] C.T. Kresge, M.E. Lenowicz, W.J. Roth, J.C. Vartuli, J.S. Beck, Nature 359 (1992) 710.
[22] J.S. Beck, J.C. Vartuli, W.J. Roth, M.E. Leonowicz, C.T. Kresge, K.D. Schmitt, C.T.W. Chu, D.H. Olson, E.W. Sheppard, S.B. McCullen, J.B. Higgins, J.L. Schlenker, J. Am. Chem. Soc. 114 (1992) 10834.
[23] N.R.E.N. Impens, P. van der Voort, E.F. Vansant, Micropor. Mesopor. Mater. 28 (1999) 217.

[24] F. Fajula, A. Galarneau, F.D. Renzo, Micropor. Mesopor. Mater. 82 (2005) 227.
[25] S. De, V.K. Aswal, P.S. Goyal, S. Bhattacharya, J. Phys. Chem. 100 (1996) 11664.
[26] Q. Huo, D.I. Margolese, U. Ciesla, P. Feng, T.E. Gier, P. Sieger, R. Leon, P.M. Petroff, F. Schuth, G.D. Stucky, Nature 368 (1994) 317.
[27] Q. Huo, R. Leon, P.M. Petroff, G.D. Stucky, Science 268 (1995) 1324.
[28] P. Van Der Voort, M. Mathieu, F. Mees, E.F. Vansant, J. Phys. Chem. B 102 (1998) 8847.
[29] J. Hu, L. Zhou, H. Li, W. Li, H. Liu, Y. Hu, Acta Phys. Chim. Sin. 21 (2005) 1217.
[30] Q. Huo, D.I. Margolese, G.D. Studky, Chem. Mater. 8 (1996) 1147.
[31] H. Kao, H. Wu, Y. Liao, A.S.T. Chiang, Micropor. Mesopor. Mater. 86 (2005) 256.
[32] W. Zhao, L. Kong, Y. Luo, Q. Li, Micropor. Mesopor. Mater. 100 (2007) 111.
[33] F. Zhang, Y. Yan, Y. Meng, Y. Xia, B. Tu, D. Zhao, Micropor. Mesopor. Mater. 98 (2007) 6.
[34] Q. Chen, Y. Wei, Y. Shi, H. Liu, Y. Hu, J. East China Univ. Sci. Technol. 29 (2003) 33.
[35] K. Wohl, Trans. AIChE 42 (1946) 215.
[36] S.I. Sandler, Chemical and Engineering Thermodynamics, Wiley, 1977, p. 363.
[37] J.J. Van Laar, Z. Phys. Chem. 72 (1910) 723.
[38] E. Alami, G. Beinert, P. Marie, R. Zana, Langmuir 9 (1993) 1465.